International Journal of Pressure Vessels and Piping 200 (2022) 104791

Contents lists available at ScienceDirect

International Journal of Pressure Vessels and Piping

journal homepage: www.elsevier.com/locate/ijpvp

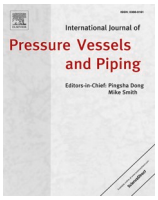

Probabilistic risk assessment for the piping of a nuclear power plant: Uncertainty and sensitivity analysis by using SINTAP procedure

Gaojun Mao [a,*], Markus Niffenegger [a], Xiuli Mao [b]

[a] Paul Scherrer Institut, Nuclear Energy and Safety Department, Structural Integrity Group, CH-5232, Villigen PSI, Switzerland
[b] Institute of Water Resources and Hydropower Research, Northwest A&F University, 712100, Yangling, China

ARTICLE INFO

Keywords:
Pipe
SINTAP
Failure probability
Sensitivity analysis
Inspection strategies

ABSTRACT

For the purpose of probabilistic fracture mechanics estimation in the field of reliability analysis of pressure vessels and piping, a probabilistic method by using SINTAP (**S**tructural **INT**egrity **A**ssessment **P**rocedures for European Industry) is developed. Monte Carlo simulation (MCS) is applied to investigate the influence of both the uncertainties of random parameters and inspection strategies on the failure probability (FP). A sensitivity analysis with regard to the above-mentioned aspects is conducted to identify the most significant parameters and efficient countermeasures to reduce failure risk in specially-assumed cases. The results of this study point out that the thickness and the inner radius of the pipe have the strongest impact on the FP of the pipe, followed by the bending moment, weld residual stress (WRS), crack length, initial crack depth, yield strength (YS), ultimate tensile strength (UTS), flow strength, fracture toughness, inner pressure and axial force. Compared with the detection quality and the inspection start time, selecting an appropriate inspection interval is a more effective method to reduce the failure risk. All these results provide a reference for the design of piping systems and guide the selection of in-service inspection (ISI) strategies with suitable flaw-detection capabilities and inspection frequencies.

1. Introduction

As clean energy sources, which produce low levels of greenhouse gas emissions, are vastly demanding, nuclear power is fully qualified for this role owing to its excellent ecological compatibility and sustainability as well as its ability to supply stably large amounts of energy. However, with increasing number of nuclear power plants (NPPs), their safe operation is a growing public concern, especially after the serious consequences of the Chernobyl and Fukushima incidents. Therefore, it is significant to analyze the reliability of structural components such as nuclear pressure vessels or piping in safety evaluations for life-time operation of NPPs [1].

In general, there are two typical methods applied for assessing the safety of the components, namely, the deterministic and the probabilistic methods. These methods focus mainly on the damage mechanisms fatigue and stress corrosion cracking (SCC) as well as the corresponding countermeasures, which should be taken by the operator [2]. The advantage of the deterministic approach owes to its simplicity and the capability of being applied relatively easily to an entire component [3]. However, the deterministic approach fails to handle with the inaccuracies in the input data needed for the integrity assessment, which is likely to cause an overestimation of the genuine "risk" related to current components operation. In brief, a purely deterministic approach provides an incomplete picture of reality. For example, both upper bound values of loads and lower bound values of material properties lead to a conservative assessment. Note that the randomness or uncertainties of the parameters should be considered for more realistic and reasonable assessment. Therefore, it is necessary to apply probabilistic methods to quantify safety margins in terms of FP [4]. For example, Cho et al. developed a systematic framework to model severe accident management guidelines into Level 2 probabilistic safety assessment of a NPP [5]. Bui et al. established an algorithm for enhancing spatiotemporal resolution of probabilistic risk assessment to address emergent safety concerns in NPPs [6]. Some probabilistic analyses have been conducted to predict the stability of piping systems during past decades. For example, Zhou et al. developed a probabilistic method for the fracture analysis of pressure piping containing circumferential defects based on the ASME (The **A**merican **S**ociety of **M**echanical **E**ngineers) procedure [7]. Qian et al. proposed a probabilistic fracture assessment method of piping systems based on FITNET FFS procedure [8]. Meanwhile, Fleming et al. made a progress in developing pipe failure

* Corresponding author.
E-mail address: gaojun.mao@psi.ch (G. Mao).

https://doi.org/10.1016/j.ijpvp.2022.104791
Received 21 June 2022; Received in revised form 8 August 2022; Accepted 30 August 2022
Available online 10 September 2022

Nomenclature

SINTAP	**S**tructural **INT**egrity **A**ssessment **P**rocedures for European Industry
MCS	Monte Carlo simulation
FP	failure probability
WRS	weld residual stress
YS	yield strength
UTS	ultimate tensile strength
ISI	in-service inspection
NPP	nuclear power plant
SCC	stress corrosion crack
ASME	The American Society of Mechanical Engineers
POD	probability of detection
FAD	failure assessment diagram
SIF (K_I)	stress intensity factor
PROST	probabilistic structure analysis code of GRS
LSF	limit state function
DMW	dissimilar metal weld
NOC	normal operation condition
MV	mean value
SD	standard deviation
CoV	coefficient of variation
OFAT	One-factor-at-a-time

databases that contain the quantity and quality of information needed to support piping system reliability evaluations [9]. Reyes-Fuentes et al. developed a new application software, AZRUSIA, for uncertainty and sensitivity analysis for nuclear reactors and calculated correlation coefficients for global sensitivity measures [10]. Because global sensitivity analysis might be insufficient to capture the influence of the inputs on a restricted domain of the output, Marrel et al. defined target and conditional sensitivity analysis to measure respectively the influence of the inputs on the occurrence of the critical event [11]. There are several approaches used for PFM models. North American and Asian codes tend to favor the elastic-plastic modeling or net section collapse models. European regulators for a large part rely in failure assessment diagram (FAD) methods for determining failure. We will focus on the latter approach. We will examine the current state-of-the-art in FAD analyses and provide no comparison between the two approaches in this paper. Since only several parameters were addressed as random variables in these assessments. One possible reason that only few variables were considered as random lies on the negative side of the probabilistic method, which is intensive, time-consuming and very complex. Therefore, it is helpful to conduct a systematic sensitivity analysis of random variables to identify the most important variables; this provides a superior basis for the risk management and would therefore help to maximize both safety and business performance. However, it's worth mentioning that for a given piping system, special attention has to be paid to the loads because they are often the only parameters which can be adjusted. WRSs, e.g. due to repair welding should be considered although they are often not known to the same degree of precision as thermal, pressure and other operation stresses. It is important thus that the sensitivity calculations reflect this uncertainty by allowing a suitably wide range of variation of these parameters [12]. To assure that the results are dependent on the existence of a crack, no initiation model will be considered in this analysis.

In addition to aforementioned assessment methods, selecting appropriate ISI strategies is also an effective method to avoid the occurrence of leakage and even the rupture of nuclear components. For example, Fleming applied Markov models for evaluating risk-informed ISI strategies for NPP piping systems [13]. Ellyln investigated the dependence of total reliability on both periodic inspection and continuous inspection programs and demonstrated the advantage in detecting small relative flaw sizes in the initial periodic inspection [14]. Nevertheless, the probabilistic approach based on the fracture module of the SINTAP procedure [12], which was agreed by a consortium of 17 European establishments under the European Union Brite-Euram Fourth Framework Scheme for the assessment of the integrity of structures, in conjunction with the consideration of ISI strategies, has not yet been comprehensively investigated.

Therefore, based on the fracture module of the SINTAP procedure and assuming the involved parameters as random variables, this paper aims to apply an improved probabilistic approach to predict the reliability of a piping system. It is organized as follows. Section 1 is dedicated to the introduction and to the state of the art of FAD methodologies for leak and rupture failures as used in many of the European applications for nuclear power plant piping. The SINTAP procedure is presented in Section 2. Section 3 deals with the probabilistic models while a presentation of the parameters is done in Section 4. Section 5 is dedicated to case studies, in which first a sensitivity analysis is performed to rank the importance of parameters affecting the failure probability of pipes by considering fatigue. In a second part of the case study, the effect of ISI (frequency and quality) on reducing the FP of piping is investigated. Finally, SSC is also considered as an important damage mechanism, thereby generating a broad base of data suitable for developing risk-informed ISI plans. The results are discussed in Section 6. The conclusions in Section 7 close the paper.

2. Failure module of SINTAP procedure

The SINTAP procedure provides seven analysis levels (i.e. one default level, three standard levels and three advanced levels) in the fracture module corresponding to different input parameters. In view of the YS mismatch between base metal and weld metal more than 10%, Level 0 (default) and Level 2 (standard) are considered in this study. Note that Level 1 will not be introduced here, as it is available for the case where the YS mismatch is less than 10%. In the SINTAP procedure, the FAD is used as an integrity rating as [15]:

$$f_{\mathrm{FAD}} = f(L_r), with \begin{cases} K_{\mathrm{r}} = \dfrac{K_{\mathrm{I}}}{K_{\mathrm{IC}}} \\ L_r = \dfrac{\sigma_{\mathrm{applied}}}{\sigma_{\mathrm{limit}}} \end{cases} \tag{1}$$

where f_{FAD} represents the failure assessment line in FAD diagram. K_{r} is the ratio of the applied stress intensity factor (SIF) K_{I} to the material's fracture toughness K_{IC} and L_{r} is equal to the ratio of applied stress $\sigma_{\mathrm{applied}}$ to the limit stress σ_{limit}, which is the YS.

Fig. 1 illustrates Eq. (1). If the assessment point falls within the non-critical region enclosed by the line of the FAD (e.g. point A in Fig. 1), the failure of the structure does not occur even if it contains cracks. In other words, the component is considered as safe if $K_{\mathrm{r}} < f(L_r)$ and this is acceptable. Inversely, the structural component is regarded as unsafe if $K_r \geq f(L_r)$ e.g. points B and C in Fig. 1. Details of the FAD approach are given in the SINTAP procedure. The shape of the function $f(L_r)$ depends on the material properties and the "level" defined. Levels 0 and 2, which are relevant in this paper and widely-accepted in the fracture mechanics community, are presented below.

2.1. Level 0

According to Level 0 of the fracture module in the SINTAP, this level requires the least information and causes the poorest accuracy. $f(L_r)$ is written as [16]:

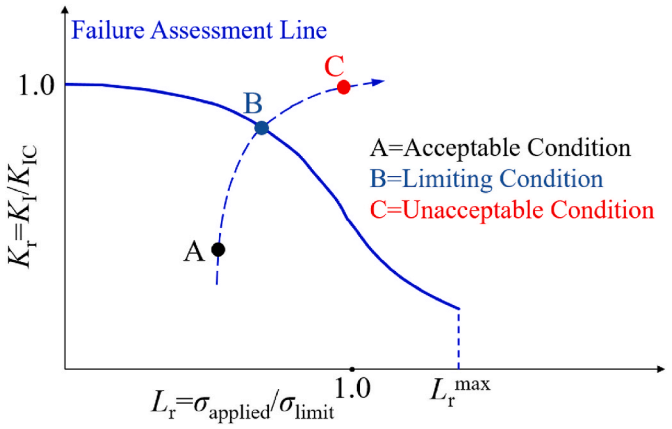

Fig. 1. Failure assessment diagram in SINTAP.

$$f(L_r)=\begin{cases}\left(1+0.5L_r^2\right)^{-\frac{1}{2}}\left[0.3+0.7e^{-\frac{1}{2}L_r^6}\right] & if\ L_r\le L_r^{max}\\ 0 \quad if\ L_r>L_r^{max}\end{cases} \tag{2}$$

where

$$L_r^{max}=\frac{1}{2}\left(1+\frac{\sigma_u}{\sigma_y}\right) \tag{3}$$

where σ_u and σ_y are UTS and YS, respectively.

2.2. Level 2

The SINTAP Level 2 analysis is implemented to deal with welding structure, where the YS mismatch between the base metal and the weld metal is over 10%. Specifically, the YS mismatch ratio M is defined as $M=\sigma_{yield}^{weld}/\sigma_{yield}^{base}$. Then the function $f(L_r)$ is given by Ref. [12]:

$$f(L_r)=\begin{cases}\left(1+0.5L_r^2\right)^{-\frac{1}{2}}\left[0.3+0.7e^{-\mu^M L_r^6}\right] \ if\ L_r\le 1\\ f(1)L_r^{\frac{N^M-1}{2N^M}} \quad if\ 1\le L_r\le L_r^{max}\\ 0 \quad if\ L_r>L_r^{max}\end{cases} \tag{4}$$

where μ^M and N^M denote the μ-parameter for the effective mismatch metal and the effective strain hardening exponent, respectively, given as [12]:

$$\mu^M=\frac{M-1}{\left(\frac{F_Y^M}{F_Y^B}-1\right)(\mu^W)^{-1}+\left(M-\frac{F_Y^M}{F_Y^B}\right)(\mu^B)^{-1}} \tag{5}$$

$$N^M=\frac{M-1}{\left(\frac{F_Y^M}{F_Y^B}-1\right)(N^W)^{-1}+\left(M-\frac{F_Y^M}{F_Y^B}\right)(N^B)^{-1}} \tag{6}$$

where F_Y^M and F_Y^B denote the limit load of the mismatch metal and the base metal, respectively. The values of μ^W, μ^B, N^W and N^B can be found in Ref. [12]. Meanwhile the maximal L_r is given by Ref. [12]:

$$L_r^{max}=\frac{F_Y^M}{F_Y^B}\times\min\left\{L_r^{maxW},L_r^{maxB}\right\} \tag{7}$$

where L_r^{maxW} and L_r^{maxB} denote the maximal L_r ratio of the weld metal and the base metal, respectively. Level 2 is able to provide more details in the region where $L_r\ge 1$ than Level 0, which can obtain a more accurate result.

3. Probabilistic models

The application of deterministic fracture mechanics assessment procedures to the prediction of fitness-for-purpose requires the use of data that are often subject to considerable

Uncertainties. An alternative approach to pure deterministic assessment is the application of structural integrity procedures such as SINTAP, in combination with probabilistic methods. The SINTAP procedure is incorporated into PROST (**PRO**babilistic **ST**ructural mechanics, a computing code developed the German Gesellschaft für Anlagen-und Reaktorsicherheit GmbH) to calculate the FP by the limit state function L_{LSF}, defined by the difference between $f(L_r)$ and K_r, given by Ref. [17]:

$$L_{LSF}=f(L_r)-K_r \tag{8}$$

If $L_{LSF}\le 0$, failure occurs. Inversely, the structure will operate safely if $L_{LSF}>0$. The FP $P_{failure}$ of a structure can be evaluated by a multi-dimensional integral (Eq. (9)) [17]:

$$P_{failure}=P(L_{LSF}\le 0)=\iint_{L_{LSF}\le 0}P(L_r,K_r)dK_r dL_r, \tag{9}$$

where $P(L_r,K_r)$ is the joint probability density of L_r and K_r. This integral is very difficult even impossible to solve by numerical integration as there are so many random parameters. Therefore, MCS method is applied to predict the FP, owing to the strong capability of handling practically every possible problem regardless of its complexity [18–20]. Based on MCS, the FP can be expressed as:

$$P_{failure}=\frac{1}{N}\sum_{i=1}^{N}x_i\ with\ x_i=\begin{cases}1, & L_{LSF}\le 0\\ 0, & others\end{cases} \tag{10}$$

where N is the total number of random parameter samples and $x_i=1$ if failure is calculated for the given parameter sample, else $x_i=0$. $\sum_{i=1}^{N}x_i$ is the total number of calculated MCS cycles resulting in $L_{LSF}\le 0$.

The flow chart in Fig. 2 shows the applied procedure for the calculation of FPs.

4. Parameter definition

4.1. Determination of SIF

For a semi-elliptical internal circumferential surface crack in a cylinder loaded by axial force and bending moment, as shown in Fig. 3, the relevant stress acting normal to the crack plane, is a superposition of stress distribution described by a fourth order polynomial as a function of the radial coordinate [21]:

$$\sigma=\sigma(y)=\sum_{i=0}^{3}\sigma_i\left(\frac{y}{a}\right)^i\ for\ 0\le y\le a \tag{11}$$

where the co-ordinate y is defined in Fig. 3 and σ_i (i = 0 to 3) are coefficients, usually fitted to results from finite element calculations, that define the axial stress state σ. The SIF is [21]:

$$K_I=\sqrt{\pi a}\left[\sum_{i=0}^{3}\sigma_i F_i\left(\frac{a}{t},\frac{2c}{a},\frac{R_i}{t}\right)+\sigma_{M_b,max}F_{M_b,max}\left(\frac{a}{t},\frac{2c}{a},\frac{R_i}{t}\right)\right] \tag{12}$$

where $\sigma_{M_b,max}$ is the maximum bending stress, namely, the maximum outer fibre bending stress. σ and $\sigma_{M_b,max}$ are the normal stresses acting at the prospective crack plane in the uncracked cylinder. For the bending moment applied along the x axis, the maximum outer fibre tensile bending stress occurs at location C as shown in Fig. 3. The coefficients F_i (i = 0 to 3) and $F_{M,max}$ are geometry functions which are given in the report [21] for the deepest point of the crack front (A), and at the

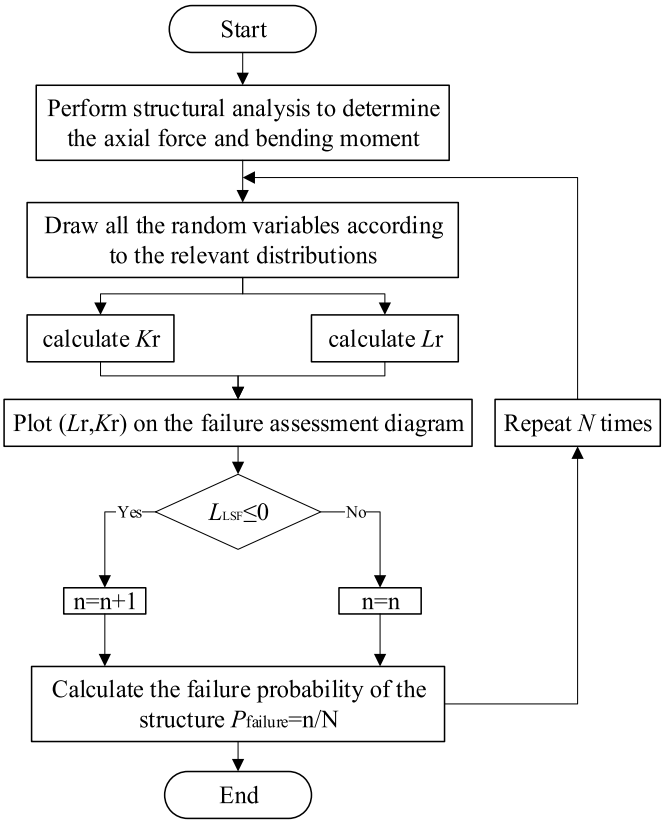

Fig. 2. The flow chart of FP calculation.

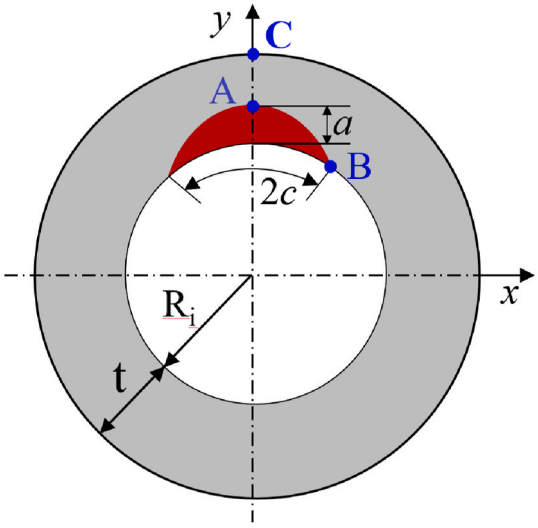

Fig. 3. Part circumferential internal surface crack in a cylinder.

intersection of the crack with the free surface (*B*), respectively in Fig. 3 to "More details are given in Ref. [22].

4.2. Determination of limit load

For homogeneous pipes and welds with defects, PROST considers the R6 [21] and FKM (Kiefner) [23] codes. Here the plastic limit stress proposed by Kiefner et al. [24] for a circumferential semi-elliptical inner surface cracks in a cylinder is used, wherein only a uniform stress value is taken into account. Meanwhile, the involved variables are considered as random variables characterized by a certain distributional function.

4.3. Uncertainty of the mechanical properties

It is a fact that the involved parameters (mechanical properties, geometry, loads, etc.) of a structure usually show a scatter, therefore called random parameters. In our calculation, the following parameters are treated as random parameters:

K_{IC}

σ_y

σ_u

- initial crack size
- loadings during normal operating condition
- pipe geometry and size

The parameters are assumed to be independent from each other and follow the normal distribution; e.g. the normal probability density of the fracture toughness K_{IC} has the form:

$$f_{K_{Ic}}(x) = \frac{1}{\sigma_{K_{Ic}}\sqrt{2\pi}} \exp\left[-\frac{1}{2}\left(\frac{K_I - \mu_{K_{Ic}}}{\sigma_{K_{Ic}}}\right)^2\right] \tag{13}$$

where $\mu_{K_{Ic}}$ and $\sigma_{K_{Ic}}$ represents the mean value and standard deviation of K_{IC}, respectively. K_I is the SIF.

5. Case study

A pipe in a NPP with a circumferential dissimilar metal weld (DMW) is selected to investigate its FP when it serves under the normal operating conditions (NOCs), including the inner pressure (7.34 MPa), temperature (290 °C), bending moment (432.6 MN mm) and axial force (159.5 kN). Note that these values in the bracket are nominal values. In addition, the WRS distribution calculated along the centerline (indicated by a dark arrow in Fig. 4(a)) in the weld metal in Fig. 4(b) is considered. It is assumed that the initial crack is located in the root center of the DMW, which suffers axial force and bending moment caused by different loadings as shown in Table 1. The initial crack is due to weld fabrication and is conservatively regarded as a surface breaking defect at the inner wall of the pipe, i.e. the crack growth is assumed to occur in the weld metal as shown in Fig. 4(a). Note that the formation of the initial crack is not considered but only its growth due to cyclic stress (fatigue) is taken into account. In our calculations with PROST, we applied the SINTAP approach to calculate fatigue crack growth, even it is not approved for fatigue load. The random variables, i.e. pipe and crack sizes according to Ref. [25], the fracture toughness, the YS and the UTS of weld metal and base metal, axial force and bending moment and their distribution types, mean values (MVs) and standard deviations (SDs) are presented in Table 1. It is assumed that the ratio between SD and MV is 0.1. MCS method is applied to predict the FP of the component and conduct sensitivity analyses on the above-mentioned variables. In order to obtain reasonable results, the MCSs are repeated by 10^6 times to achieve the L_{LSF} values. Only the mechanical properties of weld metal is considered because the base metal has little influence on the FP when the WRS along the centerline is considered. This has been demonstrated in our previous publication [22].

As in Ref. [27], where a fatigue crack growth model is used in combination with a MC method for probabilistic analysis and variance decomposition with distribution parameter uncertainty, we also used the Paris-law to characterize the cyclic crack growth rate [28]:

$$\frac{da}{dN} = C(\Delta K)^m, \ \Delta K > \Delta K_{th} \tag{14}$$

where the fatigue crack growth rate coefficient $C = 1 \times 10^{-13}$ m/cycle, the fatigue crack growth exponent $m = 3.93$ and ΔK is the cyclic change

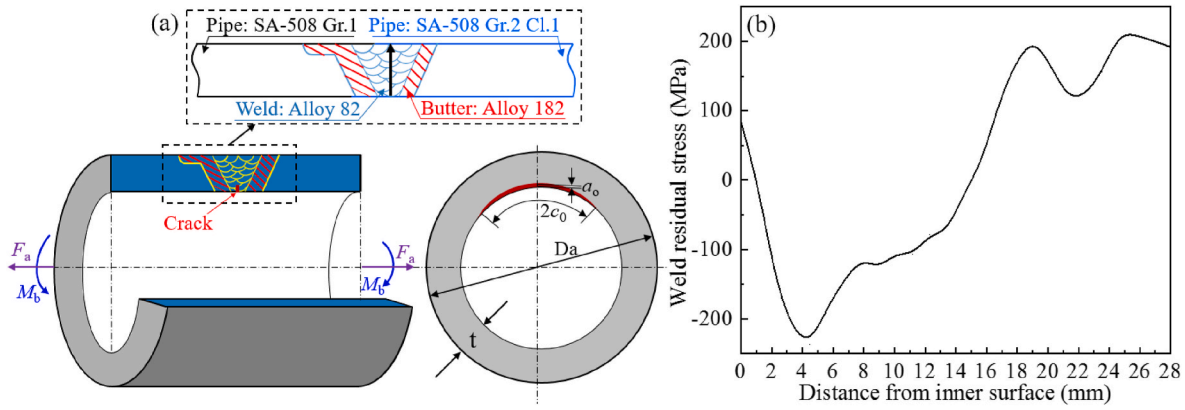

Fig. 4. Schematic illustration of straight pipe with a DMW weld.

Table 1
Main random variables used in the assessment [26].

Parameters		Distribution	Mean value	Standard deviation
Fracture toughness K_{IC} ($MPa\cdot\sqrt{m}$)	Base metal SA-508 Gr.2 Cl.1	Normal	289	28.9
	Weld metal 82/182	Normal	337	33.7
YS σ_y (MPa)	Base metal SA-508 Gr.2 Cl.1	Normal	293.2	29.3
	Weld metal 82/182	Normal	326.2	32.6
UTS σ_u (MPa)	Base metal SA-508 Gr.2 Cl.1	Normal	551.6	55.1
	Weld metal 82/182	Normal	594.2	59.4
Initial crack size	Depth a (mm)	Normal	1	0.1
	Full length $2c$ (mm)	Normal	96	9.6
Pipe size	Thickness t (mm)	Normal	28	2.8
	Outer diameter D_o (mm)	Normal	374	37.4
Bending moment M_b (MN•mm)		Normal	432.6	43.2
Force F_a (kN)		Normal	159.5	15.9
Pressure in NOC p (MPa)		Normal	7.34	0.734

in the SIF. Note that the fatigue crack growth rate $\frac{da}{dN}$ is zero if ΔK is below the threshold value ΔK_{th} (15.8 MPa $\cdot\sqrt{m}$). 30000 cycles of the bending moment and axial force are applied.

6. Results and discussion

In this analysis, a failure event is defined as a through-wall crack leading to a leakage. As the formation of a through-wall crack is a precursor event for the occurrence of a pipe breaks, the prevention of pipe leaks will also avoid pipe breaks. In the following, a sensitivity analysis is conducted to reveal the influence of variables and the effect of inspection strategies on the FP.

6.1. FPs obtained by different SINTAP levels

Regarding the uncertainty degree of random variables, a coefficient of variation (CoV) is defined by the following formula,

$$\mathrm{CoV} = \frac{\sigma}{\mu}, \tag{15}$$

where σ is the standard deviation (SD) and μ is the mean value (MV).

In a sensitivity analysis, the FP of the component shown in Fig. 4(a) for different CoVs of variables is computed by changing their SD and keeping their MV constant. By assuming M_b with a normal distribution and other variables constant, similar FPs with CoVs lower than 0.5 are obtained by considering Level 0 and Level 2. The FPs according Level 0 are lower than those according Level 2 when the CoV is larger than 0.2. This is due to the difference between Eq. (2) and Eq. (4). In addition, it is recommended to keep the best-estimate condition in mind when choosing the analysis level. On one hand, in practice the choice of level is likely to depend on other factors like the availability of materials data. Nevertheless, from the point of view of assessing appropriate margins, it is important that any excessive conservatisms or possible non-conservatisms in the analysis are recognized and accounted for. On the other hand, as the difference in σ_y between weld metal and base metal is larger than 10%, selecting Level 2 can reduce conservatism. Therefore, the Level 2 of the fracture module in SINTAP procedure is applied in the following uncertainty sensitivity analysis.

6.2. Uncertainty sensitivity analysis

A two-step process is employed to quantify the uncertainties in the FPs. A sensitivity study is conducted first to identify those uncertainties with the greatest effect on the results, and then a quantitative uncertainty analysis that addresses the most critical parameters is identified by the sensitivity calculations. The one-factor-at-a-time (OFAT) method, that is, selecting a base parameter setting and varying one parameter at a time while keeping all other parameters fixed, is applied to conduct the sensitivity analysis. The advantage of the OFAT method lies in the possibility to examine the model response over a wide range for each parameter [29], which can easily detect the contribution to the FP from each corresponding parameter.

6.2.1. Influence of standard deviation on the FP

In order to reveal the dependence of FPs on the SD from each parameter, every parameter's CoV varies from 0 to 0.5 by setting different SDs, provided that all other parameters' CoVs are kept constant, 0.1. Note that this analysis aims to be applied for a fleet plant. As a result, the FP is 3% for all variables when the CoV is at 0.1, as shown in Fig. 5(b). Fig. 5(b) also shows that the FP increases with increasing CoV and SD. In terms of the reason for higher FPs, it is likely that the larger SDs of random variables enhance more L_{LSF} to drop within the failure area, where the unacceptable condition is marked by point C in Fig. 1. The FP increases from 0.45% to 27.25% as the CoV(r_i) increases from 0 to 0.5 in Fig. 5(b). Since CoV(t) and CoV(r_i) are independent, their influence on the FP is similar. Regarding the FP influenced by SDs of the initial crack size, it is depicted in the inset in Fig. 5(b) that the FP only increases from 3% to around 5% with CoV($2c$) and CoV(a_0) larger than 0.3. In addition, the FP is not impacted significantly by the SDs of materials' properties, i.e. SD(σ_y), SD(σ_u) SD(σ_f) and SD(K_{IC}) nor to those of some loadings, i.e. SD(p) and SD(F). However, the FP is on a large scale

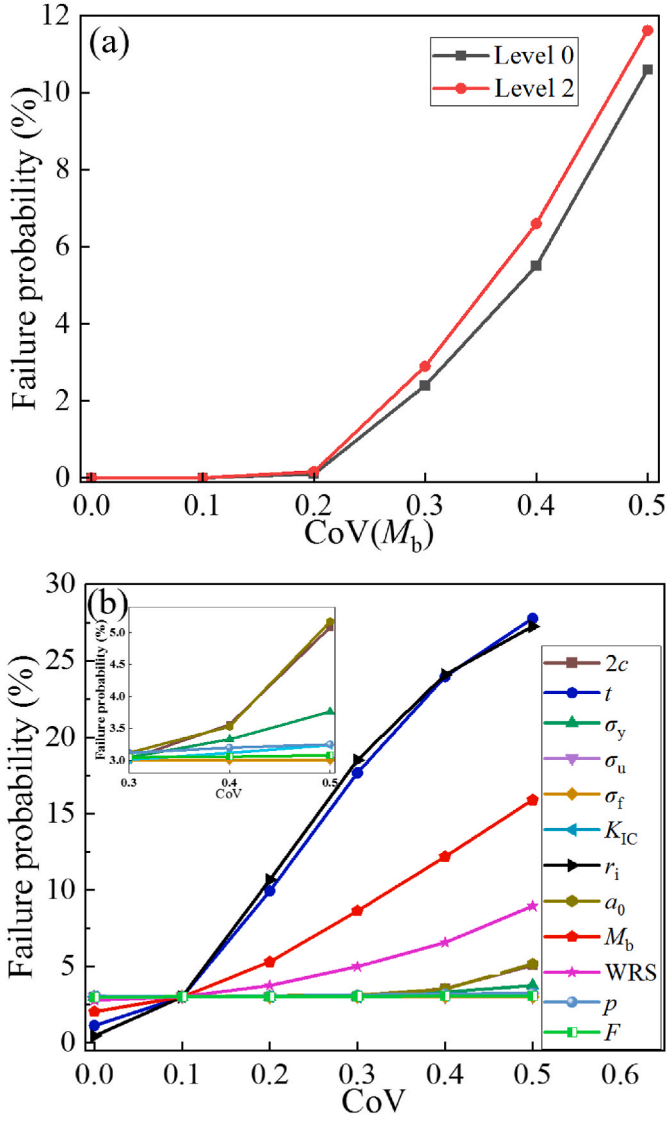

Fig. 5. (a) FP as a function of CoV (M_b) with Level 0 and Level 2. (b) Effect of CoV by changing the SD of each variable on the FP.

influenced by SDs of other loadings, including SD(WRS) and SD(M_b). The FP increases from 2.8% to 8.95% and from 2.05% to 15.9% as the CoV(WRS) and CoV(M_b) increase from 0 to 0.5, respectively. This implies that reducing SD(M_b) is more effective than reducing SD(WRS) to decrease the FP in this case.

Based on the analysis above, it is apparent that the FP of the component in this case is more sensitive to the SD of t, r_i, M_b and WRS than that of $2c$, a_0, σ_y, σ_u, σ_f, K_{IC}, p and F. Therefore, it is vital to explore their MVs to estimate the FP of this component more reasonably.

6.2.2. *Influence of mean value on the FP*

The uncertainty sensitivity is also investigated by adjusting the MV of each parameter from −50% to 50%, provided that other parameters are kept unchanged and all CoVs are set to 0.1. Taking M_b as an example, the MV and SD of M_b are multiplied by ten influential factors (i.e. 0.5, 0.6, 0.7, 0.8, 0.9, 1.1, 1.2, 1.3, 1.4 and 1.5), while other parameters remain constant. Fig. 6(a) displays the effect of varying the parameters on the FP. Apparently, the FP decreases with increasing the MVs of t, r_i and WRS. However, the FP increases with increasing the MV of M_b and varies little with the influential factors for M_b less than 0.9. The FP also increases with increasing the MVs of p, a_0, $2c$ and F, as shown in Fig. 6 (b). The tiny FP contribution from p and F is attributed to the smaller

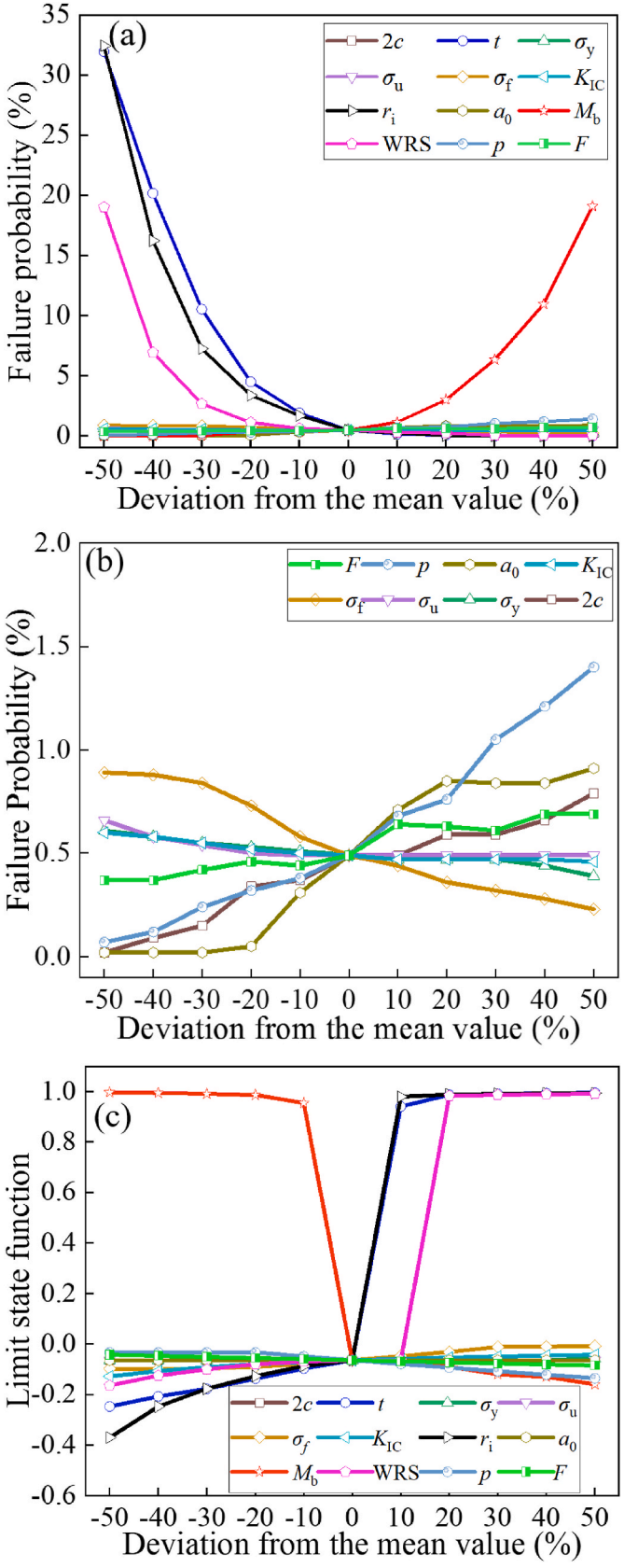

Fig. 6. (a) Effect of the variation of parameters' MV on the FP, (b) an enlarged view of the lower zone in (a), and (c) Effect of the variation of parameters' MV on the L_{LSF}.

stress caused by p and F compared with M_b. Therefore, the FP in this case is most affected by the MV of the thickness t and the inner diameter r_i of the pipe, followed by M_b, WRS, p, a_0, $2c$, σ_f and F. This finding is similar to the influence of SDs of main parameters, Therefore, a sequence of t, r_i, M_b, WRS, p, a_0, $2c$, σ_f and F should be prioritized to reduce the FP by considering their MVs. As mentioned in Eqs. (8)–(10), the FP distribution is related to L_{LSF}. The L_{LSF} distribution along the MVs of all variables is displayed in Fig. 6(c). In accordance with the variation trend of FPs in Fig. 6(a), the LSF increases by increasing the MV of t, r_i, WRS, σ_f etc., but decreases with increasing the MV of M_b, p and F. As a secondary stress, the WRS mainly act as a compressive stress shown in Fig. 4(b), so the reducing mean value of WRS is beneficial for the reduction of FP. When the MV of WRS is increased, the contribution to the FP is limited due to large bending moment. Note that only primary loadings can be adjusted in a given pipe system to reduce the FP. Moreover, the influence of p and F on the sensitivity of the FP would be increased if their MV would be higher or near the critical value.

6.2.3. Influence of CoV on the FP

As described above, the CoVs are obtained by changing SD and maintaining MV constant. In this part, the dependence of the FP on the CoVs that are obtained by changing MV and keep SD constant is also clarified. One CoV corresponds to two situations:

(1) change SD and keep MV unchanged, as shown by solid dots in Fig. 7.
(2) change MV and keep SD unchanged, as shown by hollow dots in Fig. 7.

Despite the same CoV, a big difference of the FP between these two situations can be observed. In terms of M_b as shown by red lines in Fig. 7, the FP increases with increasing CoVs obtained by increasing SDs but keeping MV a constant. On the contrary, the FP decreases with increasing CoVs obtained by reducing MV but keeping SD a constant. This difference is ascribed to the change in the overlapping region of different probability distributions caused by changing SD and MV. Therefore, both the SD and the MV of parameters should be considered in order to reduce the FP, which agrees well with the results presented in Ref. [7].

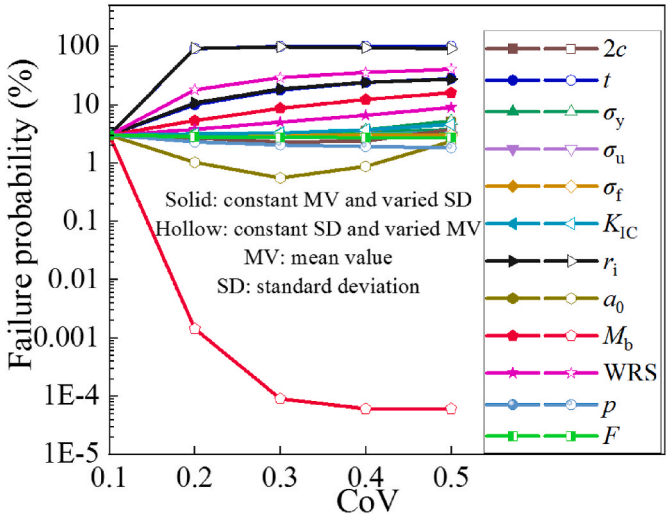

Fig. 7. Effect of CoV on the FP (Note: different CoVs are obtained by either changing SD but keeping MV a constant or changing MV but keeping SD a constant).

6.3. Influence of inspection strategies on the FP

A sensitivity study during the design and operation of piping components can help to find (efficient) ways to reduce risks related with structural failures. The failure risks obtained in the previous section were determined with no provision made for inspection. If ISI takes place, the FP will depend upon the inspection strategies. As demonstrated by a case in Ref. [30], the uncertainties of damage mechanisms play a minor role, while the inspection strategy is a key point.

6.3.1. FP variation by considering fatigue

This section presents the results of parametric calculations to predict the effects of ISI frequency and quality on reducing the FP of the straight pipe with a DMW as shown in Fig. 4(a). As one important goal of ISI, the selected strategies should ensure reliable detection of degradation before through-wall cracks result in leaks and thereby provide desired reductions in FPs. Therefore, the inspection during the whole operation time is considered by assuming the detection quality (i.e. poor, good and advanced) at given inspection intervals of 1, 5 and 10 years and assuming the inspection start time of the 1st, the 5th and the 10th year, giving $3 \times 3 \times 3 = 27$ strategies, as shown in Table 2. Note that the ISI is assumed to be done at the end of the operation year, e.g. the strategy 1 means that, based on the poor detection quality, the inspection is conducted at the end of the first year and is repeated yearly. In case a flaw is detected, the component is assumed to be repaired to prevent the occurrence of a leak or a failure and multiple inspections are assumed to be independent of each other. Three different POD curves are selected to investigate its effect on the FP. The POD is given as a function of the crack depth and the resultant POD curves are compared in Fig. 8(a) [31]. Higher POD results from the detection with higher quality, wherein the poor POD can only reach around 60% in a wide range of crack depth.

Fig. 8(b), (c) and 8(d) show the cumulative leak probabilities for 60-year of operation as functions of inspection strategies. Fig. 8(b) depicts the FPs with inspection strategies 1 to 9 based on the POD with poor quality. It is observed that the FP increases very fast from zero to 1% within the first five years and remains stable after reaching a maximum value of 3% after approximately 20 years. When compared with the case of no-inspection, the reliability of this pipe is improved significantly in

Table 2
Inspection strategies applied to the component.

Strategy	Detection quality	Inspection interval	Inspection start time
1	Poor	1	1
2		1	5
3		1	10
4		5	1
5		5	5
6		5	10
7		10	1
8		10	5
9		10	10
10	Good	1	1
11		1	5
12		1	10
13		5	1
14		5	5
15		5	10
16		10	1
17		10	5
18		10	10
19	Advanced	1	1
20		1	5
21		1	10
22		5	1
23		5	5
24		5	10
25		10	1
26		10	5
27		10	10

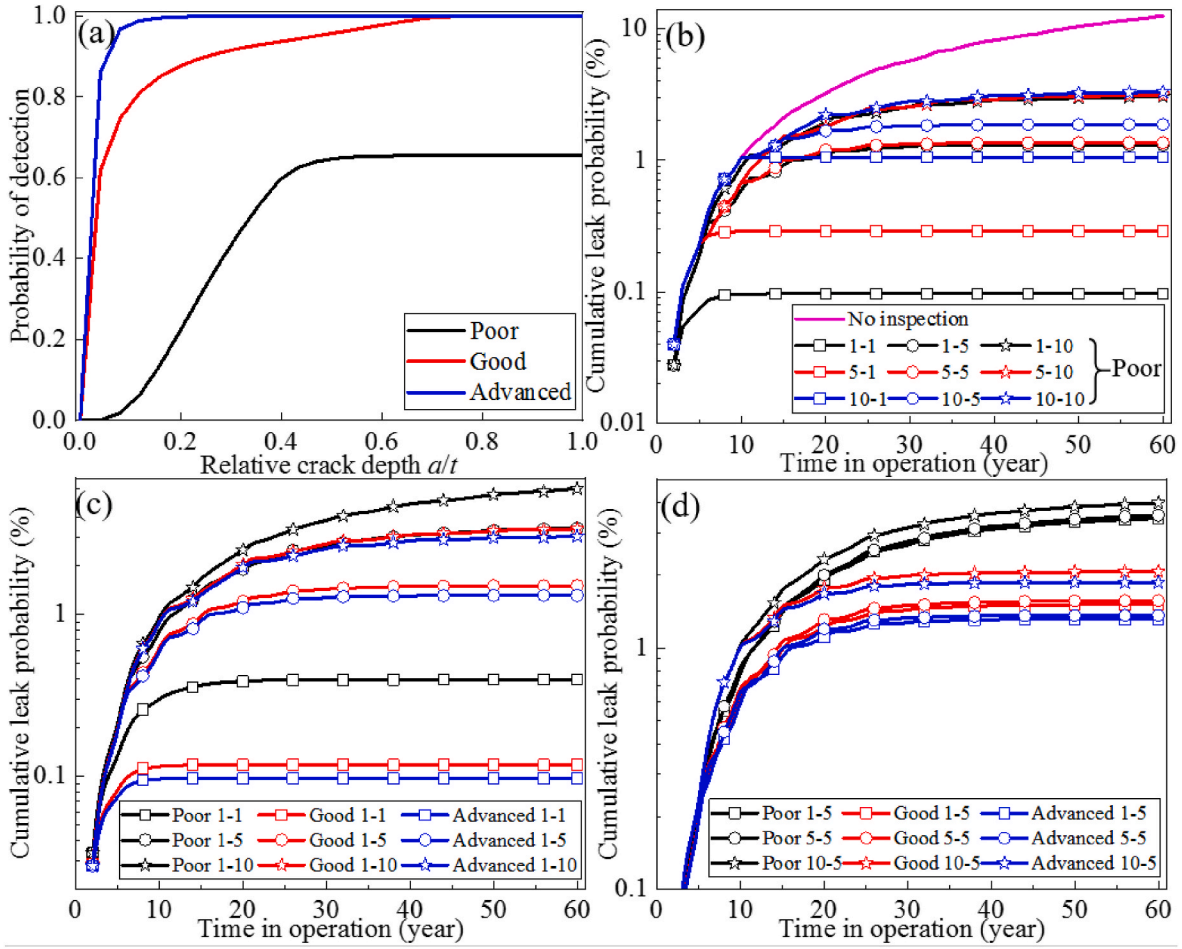

Fig. 8. (a) Probability of detection as a function of the relative crack depth, (b) Cumulative leak probability based on poor POD curves, (c) Cumulative leak probabilities with respect to three POD curves and inspection schedules 1, 2, 3, 10, 11, 12, 19, 20 and 21 over 60 years of plant operation, and (d) Cumulative leak probabilities with respect to three POD curves and inspection schedules 2, 5, 8, 11, 14, 17, 20, 23 and 26 over 60 years plant operation.

strategies 1, 4 and 7 due to the smallest ISI interval, i.e. 1 year. Fig. 8(c) displays the results obtained by considering different POD curves in conjunction with different intervals. The results in Fig. 8(c) do not indicate large differences in predicted FPs as a function of POD (only good and advanced). In other words, the detection with either good or advanced quality makes a similar contribution to reduce the FPs. In addition, the FP based on the ISI interval of 5 years and poor detection quality keeps close to that based on the intervals of 10 years but good or advanced detection quality, which indicates that the reliability of the pipe is guaranteed by ISI with only low quality but higher frequency. By considering the POD curves with either good or advanced quality, the FP improves tenfold when the ISI interval increases from 1 year to 5 years. However, the FP does not increase significantly when the ISI interval increases from 5 years to 10 years. This also demonstrates that it is more effective to decrease the inspection interval than to increase its quality to reduce the FPs. Therefore, an advanced detection capability does not offset the impact of an untimely inspection.

Although 27 ISI strategies for pipes are assumed, it is apparent that some strategies are not realistic, e.g. the strategies with yearly inspection, because e.g. in NPPs, the ISI is usually performed during the planned power outages. Therefore, we fix the interval of 5 years and take different start times and different detection qualities into consideration. As shown in Fig. 8(d), the FP obtained from poor detection is the highest, regardless of various start times. When the detection with either good or advanced quality is applied, the FP with the start time at the 1st year or the 5th year is lower than that with the start time at the 10th year, indicating that the leakage probably occurs in the range of the 5th and the 10th year. This can also be illustrated by the observation that the FP obtained from the detection with advanced quality is lower than that based on good quality, regardless of the start time, e.g. at the 1st year or the 5th year. Hence, the largest reduction (one order of magnitude) of the failure probability is predicted for the ISI with "advanced" POD and an inspection interval of one year. This conclusion agrees well with the calculations by Khaleel et al. that high-quality ISIs can be effective in reducing leak and break probabilities, particularly if the inspections were performed relatively frequently [14].

6.3.2. *Influence of SCC on FP*

Because the postulated degradation mechanism of the analyzed piping weld is fatigue, the cumulative leak probabilities in Fig. 8 are apparently small although different POD curves and inspection schedules are considered. Since SCC is a very important degradation mechanism, it is considered in the following to investigate the cumulative leak probabilities of this piping system, wherein all inspection strategies in Table 2 are reconsidered. Here we assume and apply the Nulife Alloy82 crack growth model for weld metals [32,33]:

$$\frac{da}{dt} = A \times K_I^{1.6} \tag{16}$$

where K_I is the SIF calculated in Eq. (12), the pre-factor A (mm/s) is set as 1.2×10^{-9} [22].

Fig. 9 summarizes the FPs based on 27 strategies after 60-year service of the component with the consideration of SCC. Apparently, the ISI with the poor detection quality result in higher leak probabilities, whereas

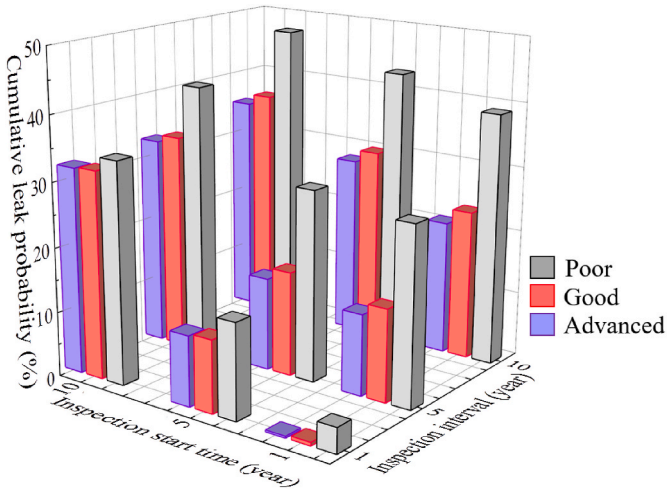

Fig. 9. Cumulative leak probabilities with respect to 27 inspection sceneries after 60-year service of the component.

such with good and advanced quality lead to similar lower leak probabilities, regardless of the start time and the interval. In other words, the inspections with "good" and "advanced" POD enhances the reliability. If the inspection starts from the end of the 10th year, the influence of intervals on the FP is negligible for a detection with either good or advanced quality but is larger for the ISI with poor quality. The FP is increased by the detection with poor quality more than enlarging the intervals, if the first inspection starts later, i.e. the 10th year. In this vein, the detection with good or even advanced quality is able to compensate for the consequence due to less frequent inspections at earlier time; this is in agreement with the results in literature that a periodic inspection with appropriate intervals can work as efficiently as a continuous inspection [14]. However, less frequent inspection can lead to higher cumulative leak probabilities when the first inspection starts at the end of the 1st year or the 5th year regardless of the detection quality. It appears that even for "advanced" POD, frequent inspections are required to achieve significant reductions in FPs. With the application of "good" and "advanced" POD curves, the earlier inspection coupled with higher inspection frequencies (i.e. strategies 16, 17, 25 and 26) acts more efficiently to reduce the FPs compared with the first inspection at the end of 10th year with higher inspection frequencies (i.e. strategies 12, 15, 21 and 24). Therefore, frequent and early inspections (e.g. one inspection per year) can provide considerable reductions in FPs.

In order to scale the contributions from different factors, i.e. POD quality, the inspection start time and the inspection interval, to the FP, the Pearson, Spearman and Kendall rank correlation coefficients between every factor and every FP yield the influence of the individual factors on the FP. More details about these three correlations are presented in Refs. [10,34]. The 27 matrixes, corresponding to all strategies in Table 2 were defined as follows:

$$[\boldsymbol{Q}_i \boldsymbol{S}_j \boldsymbol{I}_m],$$

where $\boldsymbol{Q}_i$ ($i = 1$, 2 and 3) represents the detection quality, i.e. poor, good and advanced. $\boldsymbol{S}_j$ ($j = 1$, 5 and 10) and $\boldsymbol{I}_m$ (m = 1, 5 and 10) denotes different start times and different intervals, respectively. For example, the matrix below is used to calculate the correlation coefficient between the FP and intervals with the poor detection and with the inspection start at the end of the 5th operation year.

$$\begin{bmatrix} Q_1 & S_5 & I_1 \\ Q_1 & S_5 & I_5 \\ Q_1 & S_5 & I_{10} \end{bmatrix}$$

It is found that all Spearman and Kendall correlation coefficients are 1, but the Pearson correlation coefficient varies with different strategies as shown in Fig. 10. One possible reason for this difference is that both Spearman and Kendall correlation are non-parametric methods but Pearson correlation aims to measure the strength of a linear association between variables. Fig. 10(a), (b) and (c) depict the correlation coefficients of the "POD quality and FP", "inspection start time and FP" and "inspection interval and FP", respectively. Apparently, the lowest average coefficient in Fig. 10(a) illustrates that the FP is less sensitive to the POD quality compared with either the start time or the interval. By considering the results in Fig. 10(b) and (c), we conclude that both the start time and the interval should be considered more to reduce the FP, because the correlation coefficients in these two situations are very close. Meanwhile, we infer that selecting the appropriate inspection interval can be the most effective approach to reduce failure risk.

7. Conclusions

A probabilistic method for the fracture assessment of a pipe by using SINTAP procedure has been applied in this paper. The sensitivity of the calculated FP as a function of the uncertainties of the involved random parameters and the ISI strategies are investigated to figure out the most significant influencing parameters concerning the component failure. For the analyzed case, the following conclusions are drawn:

(1) The FP increases with standard deviations of all involved parameters, wherein the FP is more sensitive to the standard deviation of the thickness t, the inner diameter r_i, bending moment M_b and WRS than to that of the crack length $2c$, the initial crack depth a_0, YS σ_y, UTS σ_u, flow strength σ_f, fracture toughness K_{IC}, inner pressure p and the axial force F. Meanwhile, the FP is most affected by the mean value of t and r_i of the pipe, followed by M_b, WRS, p, a_0, $2c$, σ_f and F.

(2) The FP varies differently with a certain CoV due to the change in the overlapping region of different probability distributions caused by changing standard deviations and mean values. Therefore, both the standard deviations and the mean values of the parameters should be taken into consideration in order to assess the FPs. During the practical maintenance of piping, care must be taken on different parameters. However, normally only primary loadings can be adjusted in a given pipe system to reduce the failure risk.

(3) Selecting the appropriate inspection interval is more effective to reduce the failure risk than increasing the detection quality or reducing the start time.

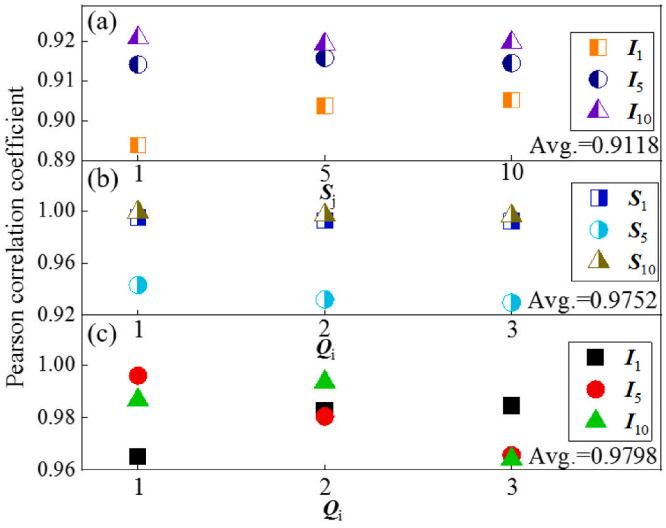

Fig. 10. Pearson correlation coefficient between inspection strategies and the leak probability.

All these results may help to lay focus on the important parameters in the design as well in the operation phase (e.g. adjustment of inspection interval) of a component to reduce failure risk. As the code (PROST) used in our analyses only considers single defects in a piping system, an optimization of coding is desirable to deal with multiple defects. Since only a single case was investigated in this paper, care should be taken of in the future work by considering several cases concurrently.

Credit author statement

G. Mao: Writing-Original draft, Visualization, Conceptualization, Data curation, Software, Formal analysis, Investigation, Methodology, Validation, Writing-Reviewing and Editing. M. Niffenegger: Project management, Supervision, Visualization, Writing-Reviewing and Editing. X. Mao: Data curation, Visualization, Validation, Writing-Reviewing and Editing. All authors have read and agreed to the published version of the manuscript.

Declaration of competing interest

The authors declare that they have no known competing financial interests or personal relationships that could have appeared to influence the work reported in this paper.

Data availability

Data will be made available on request.

Acknowledgement

The authors are grateful for the financial support of the PROBAB (Contract No. H-101247) and PROACTIV (Contract No. CTR-00489) projects provided by the Swiss Federal Nuclear Safety Inspectorate (ENSI). We thank the Gesellschaft für Anlagen-und Reaktorsicherheit (GRS) for the permission to use their PROST code and Dr. Klaus Heckmann for his continuous scientific support. We would like to thank Dr. Diego M. Mora and Mr. Hans-Peter Seifert for valuable discussions. G. Mao especially appreciate all colleagues at the Laboratory for Nuclear Materials for their kind help during his stay at PSI.

References

[1] G. Yagawa, G.W. Ye, A probabilistic fracture mechanics analysis for cracked pipe using 3-D model, Reliab. Eng. Syst. Saf. 41 (1993) 189–196.
[2] M. Modarres, I.S. Kim, Deterministic and Probabilistic Safety Analysis: Handbook of Nuclear Engineering, MA: Springer, Boston, 2010, pp. 1739–1812.
[3] K. Lawson, Pipeline corrosion risk analysis-an assessment of deterministic and probabilistic methods, Anti-corrosion Methods & Mater. 52 (2005) 3–10.
[4] J.C. Velazque, F. Calevo, J.M. Hallen, Probabilistic analysis of different methods used to compute the failure pressure of corroded steel pipelines, Int. J. Electrochem. Sci. 8 (2013) 11356–11370.
[5] J. Cho, S.H. Lee, J. Kim, S.K. Park, Framework to model severe accident management guidelines into Level 2 probabilistic safety assessment of a nuclear power plant, Reliab. Eng. Syst. Saf. 217 (2022), 108076.
[6] H. Bui, T. Sakurahara, J. Pence, et al., An algorithm for enhancing spatiotemporal resolution of probabilistic risk assessment to address emergent safety concerns in nuclear power plants, Reliab. Eng. Syst. Saf. 185 (2019) 405–428.
[7] J. Zhou, S. Shen, A study on reliability assessment methodology for pressure piping containing circumferential defects I: computation method of failure probability of welded joint containing circumferential defects, Int. J. Pres. Ves. Pip. 75 (1998) 679–684.
[8] G.A. Qian, M. Niffenegger, Probabilistic fracture assessment of piping systems based on FITNET FFS procedure, Nucl. Eng. Des. 241 (2011) 714–722.
[9] K.N. Fleming, B.O.Y. Lydell, Database development and uncertainty treatment for estimating pipe failure rates and rupture frequencies, Reliab. Eng. Syst. Saf. 86 (2004) 227–246.
[10] M. Reyes-Fuentes, E. del-Valle-Gallegos, J. Duran-Gonzalez, et al., AZTUSIA: a new application software for Uncertainty and Sensitivity analysis for nuclear reactors, Reliab. Eng. Syst. Saf. 209 (2021), 107441.
[11] A. Marrel, V. Chabridon, Statistical developments for target and conditional sensitivity analysis: application on safety studies for nuclear reactor, Reliab. Eng. Syst. Saf. 214 (2021), 107711.
[12] S. Webster, A. Bannister, Structural integrity assessment procedure for Europe- of the SINTAP programme overview, Eng. Fract. Mech. 67 (2000) 481–514.
[13] K.N. Fleming, Markov models for evaluating risk-informed in-service inspection strategies for nuclear power plant piping systems, Reliab. Eng. Syst. Saf. 83 (2004) 27–45.
[14] F. Ellyin, Reliability of piping systems and effect of inspection methods, Struct. Saf. 3 (1986) 85–99.
[15] Y.G. Matvienko, Failure Assessment Diagrams in Structural Integrity Analysis: Damage and Fracture Mechanics, Springer, Dordrecht, 2009, pp. 173–182.
[16] British Energy, Assessment of the Integrity of Structures Containing Defects: R6-Revision 4, BNFL Magnox Generation, AEA Technology, 2001.
[17] P. Dillstroem, ProSINTAP-A probabilistic program implementing the SINTAP assessment procedure, Eng. Fract. Mech. 67 (2000) 647–668.
[18] O. Ditlevsen, H.O. Madsen, Structural Reliability Methods, Wiley, Chichester, 1996, pp. 895–900. Baffins Lane.
[19] S.S. Afshari, F. Enayatollahi, X. Xu, X. Liang, Machine learning-based methods in structural reliability analysis: a review, Reliab. Eng. Syst. Saf. 219 (2022), 108223.
[20] N.D. Lagaros Nd, V. Plevris, M. Papadrakakis, Neurocomputing strategies for solving reliability-robust design optimization problems, Eng. Comput. 27 (2010) 819–840.
[21] W. Zang, Stress Intensity Factor Solutions for Axial and Circumferential through Wall Crack in Cylinders, British energy generation Ltd, Barnwood, Gloucester, 1997, pp. 25–27.
[22] G.J. Mao, M. Niffenegger, Probabilistic and deterministic investigation on single crack growth in dissimilar metal welds of a piping system, Int. J. Pres. Ves. Pip. 195 (2022), 104566.
[23] J.F. Kiefner, W.A. Maxey, R.J. Eiber, A.R. Duffy, Failure Stress Levels of Flaws in Pressurized Cylinders, ASTM International, West Conshohocken, PA, 1973, pp. 461–481.
[24] R. Rastogi, V. Bhasin, K. Vaze, H. Kushwaha, Assessment of integrity of components in piping of 500MWe PHWR: using R-6 method, Nucl. Eng. Des. 212 (2002) 109–114.
[25] M.H. Qin, D.V. Walter, KKL DMW Fracture Mechanics Evaluations, Structural integrity associates, Inc., 2014. Report No. 1300355.302, section 3.9.
[26] M.H. Qin, D.V. Walter, Material Properties for Residual Stress Analyses, Including MISO Properties up to Material Flow Stress, Structural integrity associates, Inc., 2014. Report No. 1300355.307, Appendix C.
[27] J. Mcfarlan, E. Decarlo, A Monte Carlo framework for probabilistic analysis and variance decomposition with distribution parameter uncertainty, Reliab. Eng. Syst. Saf. 197 (2020), 106807.
[28] P. Paris, F. Erdogan, A critical analysis of crack propagation laws, J. Basic Eng. 85 (1963) 528–534.
[29] D.D. Frey, R. Jugulum, The mechanisms by which adaptive one-factor-at-a-time experimentation leads to improvement, J. Mech. Des. 128 (2006) 1050–1060.
[30] K. Heckmann, R. Alzbutas, M. Wang, et al., Comparison of sensitivity measures in probabilistic fracture mechanics, Int. J. Pres.s Vessel Pip. 192 (2021), 104388.
[31] K. Heckmann, Q. Saifi, Comparative analysis of deterministic and probabilistic fracture mechanical assessment tools, Kerntechnik 81 (2016) 484–497.
[32] R.W. Bosch, S. Van Dyck, SCC Pilot Study RA3. NULIFE Report No, vol. 8, NULIFE, 2009, p. 23. https://www.scribd.com/document/386357143/Nulife-08-23-Scc-Pilot-Study-Ra-3.
[33] A. Jenssen, K. Norrgård, K. Lagerström, G. Ebring, C. Jansson, P. Efsing, Structural assessment of a defected nozzle to safe-end welds in ringhals 3 and 4, Societe Francaise d'energie nucleaire-SFEN 1175 (2002) 43–54.
[34] (https://www.statisticssolutions.com/free-resources/directory-of-statistical analyses/correlation-pearson-kendall-spearma)n/.